



LAWRENCE
LIVERMORE
NATIONAL
LABORATORY

Self-Interstitial Transport in Vanadium

L. A. Zepeda-Ruiz, J. Rottler, B. D. Wirth, R. Car,
D. J. Srolovitz

January 14, 2005

Acta materialia

Disclaimer

This document was prepared as an account of work sponsored by an agency of the United States Government. Neither the United States Government nor the University of California nor any of their employees, makes any warranty, express or implied, or assumes any legal liability or responsibility for the accuracy, completeness, or usefulness of any information, apparatus, product, or process disclosed, or represents that its use would not infringe privately owned rights. Reference herein to any specific commercial product, process, or service by trade name, trademark, manufacturer, or otherwise, does not necessarily constitute or imply its endorsement, recommendation, or favoring by the United States Government or the University of California. The views and opinions of authors expressed herein do not necessarily state or reflect those of the United States Government or the University of California, and shall not be used for advertising or product endorsement purposes.

Luis A. Zepeda-Ruiz,¹ Jörg Rottler,² Brian D. Wirth,³ Roberto Car,² and David J. Srolovitz²

¹*Chemistry and Materials Science Directorate, Lawrence Livermore*

National Laboratory, P.O. Box 808, L-371, Livermore, Calif. 94550

²*Princeton Institute for the Science and Technology of Materials (PRISM),*

Princeton University, Princeton, New Jersey 08544

³*Department of Nuclear Engineering, University of California, Berkeley, Calif. 94720*

(Dated: November 11, 2004)

We study the diffusion of self-interstitial atoms (SIAs) and SIA clusters in vanadium via molecular dynamics simulations with an improved Finnis-Sinclair potential (fit to first-principles results for SIA structure and energetics). The present results demonstrate that single SIAs exist in a $\langle 111 \rangle$ -dumbbell configuration and migrate easily along $\langle 111 \rangle$ directions. Changes of direction through rotations into other $\langle 111 \rangle$ directions are infrequent at low temperatures, but become prominent at higher temperatures, thereby changing the migration path from predominantly one-dimensional to almost isotropically three-dimensional. SIA clusters (i.e., clusters of $\langle 111 \rangle$ -dumbbells) can be described as perfect prismatic dislocation loops with Burgers vector and habit planes of $1/2\langle 111 \rangle\{220\}$ that migrate only along their glide cylinder. SIA clusters also migrate along $\langle 111 \rangle$ -directions, but do not rotate. Both single SIAs and their clusters exhibit a highly non-Arrhenius diffusivity, which originates from a combination of a temperature dependent correlation factor and the presence of very low migration barriers. At low temperature, the diffusion is approximately Arrhenius, while above room temperature, the diffusivity is a linear function of temperature. A simple model is proposed to describe these diffusion regimes and the transition between them.

Keywords molecular dynamics simulation, vanadium, interstitial, diffusion, dislocation loop

I. INTRODUCTION

The creation and evolution of point defects play an important role in determining many of the structural properties of materials. The two elementary point defects in metals are vacancies and self-interstitial atoms (SIA). Under normal conditions, vacancy concentrations are much larger than SIA concentrations in most metals. However, the creation and migration of SIAs are critical for microstructural evolution of materials in high energy radiation environments [1, 2] and in ion implantation [3]. SIAs are usually very mobile (i.e., the migration barriers for SIAs are relatively small) and, hence, play an important role in controlling the rates of several types of microstructural processes in such applications. In the present paper, we focus specifically on vanadium because of recent interest in the application of vanadium-based alloys for structural components in advanced fusion reactors [4–7].

Extensive computer simulation studies on SIAs in metals have been performed to date [8–12]. For example, simulations of bcc Fe have shown that SIAs and SIA clusters (small, perfect dislocation loops) are created along close-packed directions and tend to migrate along specific crystallographic directions. In this material, the SIAs preferentially lie in $\langle 110 \rangle$ orientations but rotate into $\langle 111 \rangle$ -directions in order to migrate. Three dimensional diffusion in such a system results from diffusion in a $\langle 111 \rangle$ direction, relaxation into a stable $\langle 110 \rangle$ orientation and then rotation into another $\langle 111 \rangle$ directions; this produces an Arrhenius temperature dependence with an

apparent activation energy of order ~ 0.1 eV [8, 9].

Simulation studies of SIA migration have also been performed for bcc vanadium [13–17]. However, these empirical interatomic potential-based simulations are not consistent with recent first principles calculations [18], which clearly show that the stable SIA structure in V is a $\langle 111 \rangle$ oriented dumbbell, rather than the $\langle 110 \rangle$ oriented dumbbell found in Fe. Given this fundamental discrepancy, SIA migration in Fe and V must be fundamentally different and our current understanding of SIA diffusion in V is rather limited. This calls for a reexamination of the relevant mechanisms.

In a recent communication [20], we undertook a molecular dynamics (MD) study of single SIA migration in V using an improved interatomic potential [19], which was fit to the point defect properties determined from the first principles calculations (and other experimental and first principles data) [18]. This work [20] revealed that the diffusivity of single SIAs does not follow the conventional Arrhenius behavior for solid state diffusion, but in fact shows strong deviations. Part of the non-Arrhenius behavior was attributed to a temperature dependent correlation factor, but the strong deviations at higher temperatures could only be rationalized in a more general framework of particles migrating over extremely small barriers. In this regime, we argued that the diffusivity varies linearly with temperature rather than Arrheniusly.

The present paper presents additional results on single SIA diffusion and extends the study to SIA clusters. We find that the arguments developed for the single SIA case

also apply to cluster diffusion. We then develop a general framework for SIA and SIA cluster migration that describes all temperature regimes correctly.

II. COMPUTATIONAL METHOD

Molecular dynamics simulations have been widely used to study point defect motion. They provide an ideal tool for understanding SIA migration, where complex local atomic rearrangements occur during the fundamental diffusional processes that are not readily captured using static simulation methods. Although first-principles MD methods, such as the Car-Parrinello method [21], provide a means of observing the dynamics of the atomic structure based upon quantum mechanical information, they are generally too computationally expensive for the simulation of a large number of transition metal atoms over sufficiently long time to extract meaningful SIA migration information. On the other hand, MD simulations based upon empirical potentials such as pair potentials or embedded-atom-method (EAM) potentials [22–26] are widely used in the study of SIA and SIA clusters [27–29]. Such calculations are more computationally efficient, yet compromise the description of atomic bonding, as compared with the first principles methods. Empirical potentials are, nonetheless, useful, provided they are able to reproduce the basic equilibrium SIA properties of interest.

In a previous study [19], we developed a Finnis-Sinclair-type (FS) empirical potential for vanadium that was fit to first-principles SIA and vacancy formation energies, structural data and a number of other equilibrium properties [18]. Both the present FS potential and the first-principles calculations indicate that the most stable SIA is a $\langle 111 \rangle$ -dumbbell, which is nearly degenerate with the crowdion configuration. Since the accuracy of the first-principles data is approximately 0.05 eV, the difference between the $\langle 110 \rangle$ -dumbbell configuration (predicted from earlier empirical potential calculations) and the $\langle 111 \rangle$ -dumbbell configuration can be considered reliable (0.34 eV).

Diffusion of individual SIAs and SIA clusters in vanadium was investigated using the MD simulation code MDCASK [30] using the FS potential for vanadium described in ref. [19]. For the case of single SIAs, all simulations were performed in a cubic system of size $2000+1$ V atoms (a $10a_0 \times 10a_0 \times 10a_0$ computational cell, where the equilibrium cubic lattice parameter $a_0 = 3.03$ Å) while for SIA clusters, the cubic system consisted of $54000+n$ (a $30a_0 \times 30a_0 \times 30a_0$ computational cell) where $n = 7, 19, 37, 61$. For these values, the SIA's will form filled concentric hexagonal shells surrounding a central SIA. These two computational supercells were tested to ensure that the effect of interactions of a single SIA or a SIA cluster with their periodic images were negligible. In addition, periodic boundary conditions were applied to effectively provide an infinite extension of the struc-

ture. Both, single SIAs and SIA clusters were introduced in the form of $\langle 111 \rangle$ -dumbbells and equilibrated for 10 ps using a canonical (NVT) ensemble, where the temperature was controlled using a Langevin thermostat. The simulation was then switched to a microcanonical (NVE) ensemble in order to study the SIA migration dynamics. Simulations were run at temperatures between 100 and 2000 K and the time step used in the integration of the equations of motion was set to 1 fs. Because of the highly correlated nature of interstitial diffusion, long simulation runs (1 ns) were required to ensure that reliable diffusivities were obtained.

III. STATIC SIA CLUSTER PROPERTIES

Our first task in the analysis of SIA and SIA-cluster diffusion in V was the correct identification of the interstitial(s) during the simulation. To this end, we divided the whole space into Wigner-Seitz (W-S) cells centered around each perfect crystal lattice site. The criterion adopted for interstitial ($\langle 111 \rangle$ -dumbbell) identification was the existence of more than one atom in the same W-S cell. Note that while this approach easily identifies dumbbells, interstitials in the crowdion geometry are not easily identified (i.e., one of the crowdion atoms sits on the cell face). To alleviate this difficulty, we enlarge the W-S by 5%. In this case, a dumbbell will exist in a single W-S cell, while a crowdion will simultaneously exist in two adjacent W-S cells.

Figure 1 shows [111] and [001] projections of clusters containing 19, 37 and 61 SIAs. The filled circles represent the centers of mass of the $\langle 111 \rangle$ dumbbell SIAs. In Fig. 1(a), the dumbbells are oriented normal to the viewing plane. The dumbbell structure is more easily seen in the [001] projection of Fig. 1(b). Examination of Fig. 1 demonstrates that the clusters are perfect prismatic dislocation loops, bounded by $a/2\langle 111 \rangle$ edge dislocation segments. However, the clusters are more extended than a perfect planar prismatic dislocation loop located on only two additional (220) planes, as shown in Fig. 1. The 19-, 37- and 61-member SIA clusters occupy five, six and eight (220) planes, respectively.

These clusters were generated by an annealing process, which involved increasing the temperature in 2ps steps of 10 K between 0 and 100 K. Between 100 and 900 K, the temperature increment was increased to 50 K. Once the final temperature was reached, the system was equilibrated for 10 ps. To obtain the zero temperature structure, the system was quenched from 900 K to 1 K, followed by a conjugate gradient minimization of the energy. All final configurations, obtained from the thermal structural relaxation, consisted of perfect dislocation loops with Burgers vector $\mathbf{b} = \frac{1}{2}\langle 111 \rangle$, regardless of initial configuration ($\frac{1}{2}\langle 111 \rangle\{110\}$, $\langle 110 \rangle\{110\}$, and $\langle 100 \rangle\{110\}$). A key feature observed from the MD simulations was that during the initial stage of the heating schedule ($0 K < T < 10 K$) initial $\frac{1}{2}\langle 110 \rangle$ or $\langle 100 \rangle$

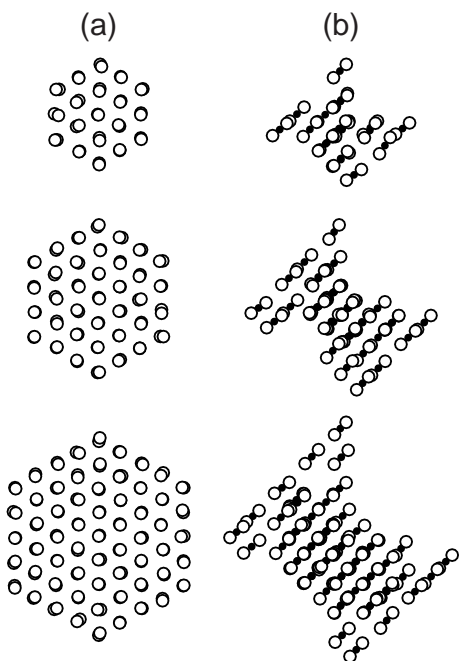


FIG. 1: 19-, 37- and 61-member SIA clusters in (a) [111] and (b) [001] projection. Filled and open circles represent the centers of mass and $\langle 111 \rangle$ -dumbbell, respectively.

loops reoriented almost immediately along a $\langle 111 \rangle$ direction [42].

IV. SINGLE SIA AND SIA CLUSTER MIGRATION

In order to investigate the migration mechanism of SIAs and SIA clusters in vanadium, we first analyze the interstitial trajectories as a function of temperature and cluster size. Representative trajectories for the single SIA and SIA cluster centers of mass, collected over 1 ns simulations, are shown in Fig. 2. Since we apply periodic boundary conditions, the dumbbells/clusters sometimes cross the cell boundary. In this case, they are translated by adding or subtracting lattice vectors such that the trajectories in Fig. 2 appear as if in an infinite solid.

Examination of Fig. 2 shows that the single SIA migration mechanism is temperature dependent. Only one-dimensional (1D) random walks are observed for temperatures from 100K to 600K during the 1ns simulation, as shown in Fig. 2(a). At $T \sim 700$ K, the SIA makes infrequent rotations from one $\langle 111 \rangle$ - to other $\langle 111 \rangle$ -directions. Such rotation events lead to three-dimensional (3D) trajectories, consisting of long 1D random walk segments with abrupt reorientations, (see Figs. 2(b-d)). With increasing temperature, the frequency of the rotation events increases and the lengths of the 1D trajectory segments decrease. On the other hand, SIA clusters

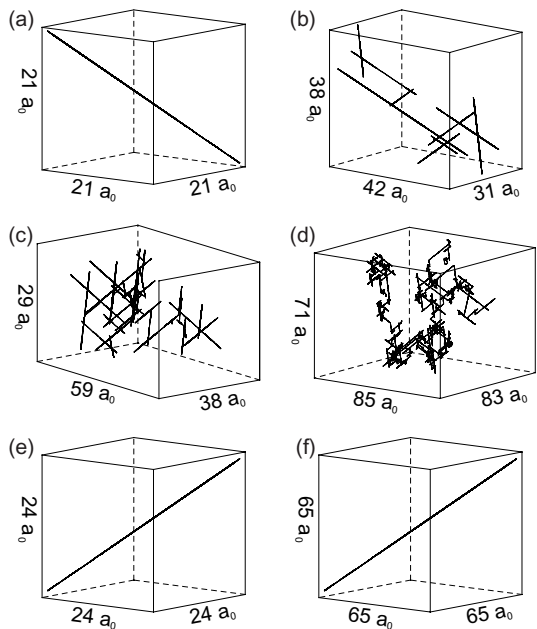


FIG. 2: Typical trajectories of migrating SIAs for temperatures of (a) 300 K, (b) 700 K, (c) 900 K and (d) 1400 K and 7-member SIA clusters for temperatures of (e) 300 K and (f) 1200 K.

undergo a collective one-dimensional migration along a $\langle 111 \rangle$ -direction (i.e., parallel to the SIA dumbbell orientations), similar to that of single SIA at low temperature. SIA cluster migration was one-dimensional for all $T < 1200$ K, as shown in Figs. 2(e) and (f). For $T > 1200$ K, the SIA clusters disintegrate into individual SIAs.

Although these results appear to be similar to those reported for other bcc metals (i.e., Fe and Mo) [8, 27, 39, 40], there is an important difference, particularly for the case of single SIAs. This difference is associated with the stable form of the interstitial: in V the equilibrium dumbbell orientation is $\langle 111 \rangle$, while Fe and Mo exhibit $\langle 110 \rangle$ -dumbbells. In the Fe and Mo cases, the dumbbell remains in a $\langle 110 \rangle$ -orientation until it is thermally activated into one of the $\langle 111 \rangle$ -directions, where it undergoes single or multiple hops before relaxing back into a $\langle 110 \rangle$ -orientation [39]. There are no relaxation events of this type in interstitial migration in V. In the V case, the stable $\langle 111 \rangle$ -dumbbell migrates long distances and only requires significant thermal activation to reorient into another $\langle 111 \rangle$ -direction. Therefore, while the dumbbell migration trajectories look qualitatively similar in the V, Fe and Mo (cf. Fig. 2(e) and Fig. 5 in Ref. [39]), they have fundamentally different origins.

Figure 3 shows a segment of the trajectory for single SIA and 7-member SIA cluster centers of mass at $T = 500$ K. It can be seen that while migration for single SIAs is discrete, i.e., it moves by jumping from one body centered cubic lattice site to another, the SIA cluster center of mass is not localized at lattice sites, but moves in

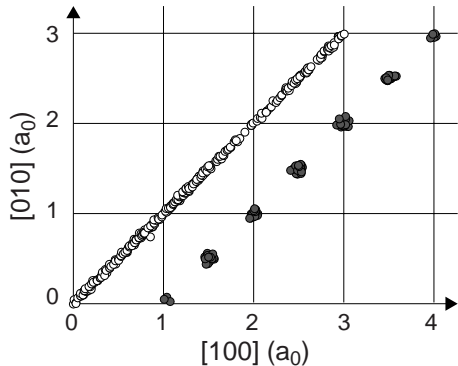


FIG. 3: A [001] projection of a segment of the single SIA (open circles) and 7-member SIA cluster (shaded circles) center of mass trajectories. The grid denotes lattice sites and the trajectories are shifted for comparison.

a more continuous manner along a $\langle 111 \rangle$ -direction. Clusters do not translate as rigid units, but rather by forming and annihilating interstitials at its periphery.

Figure 4 shows positions of the 2 SIA atoms that form the dumbbell relative to the 4 distinct $\langle 111 \rangle$ directions. Many positions are shown that are being sampled by the SIA's during the course of the simulation. We observe that at very low temperatures ($T = 100$ K, shown in Fig. 4(a)) the SIA dumbbell vibrates around the $\langle 111 \rangle$ -direction along which it migrates. The shape of the distribution (i.e., the triangular arrangement of the clustered points in Fig. 4(a)) reflects the 3-fold symmetry of the $\langle 111 \rangle$ plane. As T increases ($T = 500$ K, shown in Fig. 4b), the SIA vibrates about its $\langle 111 \rangle$ migration direction, but with a wider distribution than at 100K. Finally, for higher T (Figs. 4(c) and (d)) the SIA both samples all of the possible $\langle 111 \rangle$ -directions and does so with a distribution of a width that increases with temperature. Nonetheless, the most probable dumbbell orientations continue to lie along $\langle 111 \rangle$ directions.

To obtain a more detailed understanding of SIA migration, we monitored the rate of rotation, ω_r , from one $\langle 111 \rangle$ -direction to one of the other $\langle 111 \rangle$ -direction as a function of $1/k_B T$ for temperatures between 700 K and 1600 K (see Fig. 5). No rotations were observed at 600K or below (as expected from extrapolation of the best fit line in the figure to these lower temperatures). The logarithm of the rotation rate is a linear function of the inverse temperature. This suggests that rotation is indeed a thermally activated (Arrhenius) process. The activation energy obtained from Fig. 5, $\Delta E_r = 0.44$ eV, is consistent with first-principles calculations [18] and static calculations using the new interatomic potential [19] which predict a rotational barrier for SIAs in V of 0.35 eV and 0.4 eV, respectively [20]. The pre-exponential factor obtained from the fit is $\omega_0 = 1.3 \times 10^{13} \text{ sec}^{-1}$.

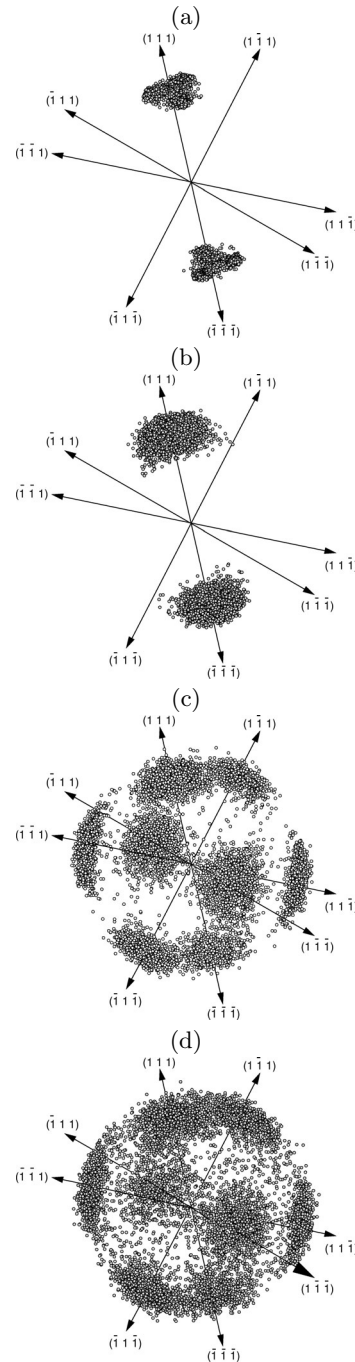


FIG. 4: Distribution of orientations of a single interstitial dumbbell at (a) 100 K, (b) 500 K, (c) 900 K, and (d) 1300 K for single SIA diffusion, where pair of points represents the dumbbell position at different times separated by 200 ns.

V. SIA AND SIA CLUSTER DIFFUSIVITY

Diffusivities were calculated following the procedure employed by Guinan *et al.* [31] The total simulation time was partitioned into m intervals of equal duration τ_i and a diffusivity $D_i = \langle R^2 \rangle / 6\tau_i$ was calculated from the

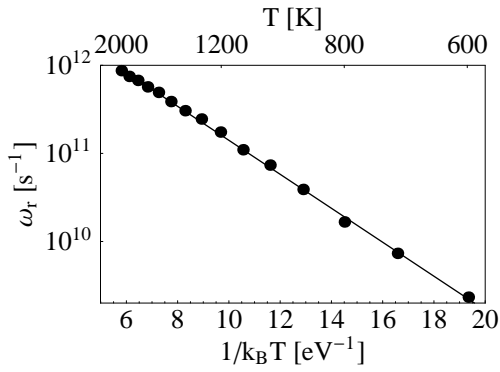


FIG. 5: Rotation rate ω_r , as a function of temperature. The solid line is an Arrhenius fit to the data with slope $\Delta E_r = 0.44 \text{ eV}$ and pre-exponential factor $\omega_0 = 1.3 \times 10^{13} \text{ sec}^{-1}$.

mean squared displacements $\langle R^2 \rangle$ of the center of mass (of either single SIA or SIA clusters) during that interval. This procedure was repeated after shifting all intervals by a time $\Delta\tau$ along the trajectory. τ and $\Delta\tau$ were chosen to ensure that the averages are uncorrelated and statistically significant. We employed τ from 5 to 100 ps with $\Delta\tau = 1 \text{ ps}$. For every value of τ_i , we thus obtain a mean diffusivity $\langle D_i \rangle$ by averaging over all values of D_i . The total diffusivity D then results from averaging over all $\langle D_i \rangle$,

$$D = \frac{1}{m} \sum_{i=1}^m \langle D_i \rangle, \quad (1)$$

We adopt the convention of treating all trajectories as 3D random walks, since rotations will also occur at the lower temperatures if the simulations were extended to longer times and the values of $\langle R^2 \rangle$ are unaffected by them. Figure 6 shows $\langle R^2 \rangle$ as a function of time for individual SIAs and SIA clusters together with linear fits to the data. All curves are consistent with purely diffusive behavior.

The computed diffusivities (from Eq. (1)) are shown in Fig. 7 for temperatures between 100 K and 2000 K for single SIAs and between 200 K and 1200 K for SIA clusters. The diffusivity increases with increasing T , but decreases with increasing SIA cluster size. This reduction in the diffusivity with increasing cluster size is not surprising in light of the observation that the clusters move by adding and removing interstitials at the cluster periphery rather than moving through a rigid body translation.

If the diffusivity were to obey the classical Arrhenius relation

$$D = \nu_0 a_0^2 \exp[-\Delta E_d/k_B T], \quad (2)$$

the data for each cluster size in Fig. 7 would lie along a straight line. This is clearly not the case; the data

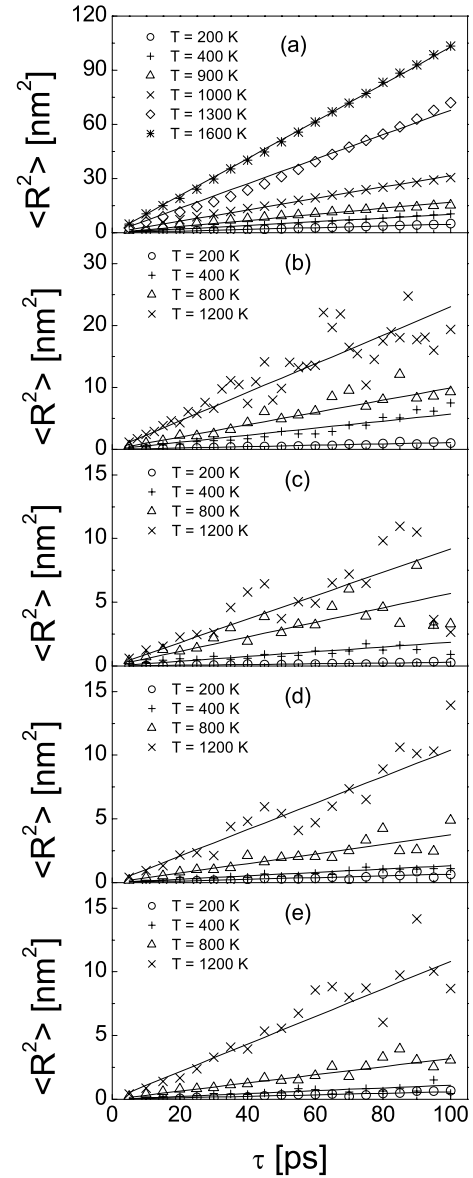


FIG. 6: Mean square displacement as a function of time for (a) individual SIAs, (b) a 7-member SIA cluster, (c) a 19-member SIA cluster, (d) a 37-member SIA cluster and (e) a 61-member SIA cluster at several temperatures

in Fig. 7 show pronounced curvature for all values of n - especially at high temperature. Although Arrhenius behavior is widely expected for diffusion in the solid state, it clearly does not occur here. Interestingly, however, all curves appear to be nearly parallel to each other in the Arrhenius plot.

The presence of a non-linear regime in the Arrhenius plot of Fig. 7 is intriguing. As discussed above, previ-

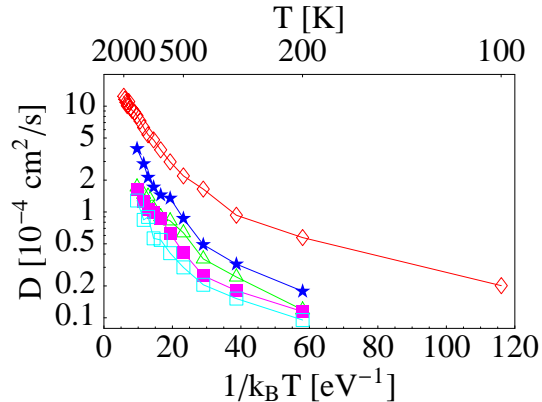


FIG. 7: Arrhenius plot of the diffusivity as calculated from Eq. (1) for single SIAs (\diamond) as well as clusters of size $n = 7$ (\star), $n = 19$ (\triangle), $n = 37$ (\blacksquare) and $n = 61$ (\square).

ous studies of SIA migration in bcc metals [8, 39] showed that SIA migration is a multiple step process that involves not only translation of $\langle 111 \rangle$ -oriented dumbbells along a $\langle 111 \rangle$ -direction, but also rotations from the stable $\langle 110 \rangle$ - to $\langle 111 \rangle$ -oriented dumbbells. One could argue that the non-linearity observed in Fig. 7 is a result of the competition (over a certain temperature regime) of these thermally activated processes. This is clearly not the situation in the case of V, since the ground state of the interstitial is the $\langle 111 \rangle$ -oriented dumbbell, and no additional rotation is required to access this easy-glide configuration. The fact that the single SIA diffusion data does not fall on a straight line in the Arrhenius plot below 700, where no rotations were observed in the simulations, proves that SIA dumbbell rotation is not responsible for the observed non-Arrhenius behavior.

A. Correlation analysis

We find that another mechanism is contributing to the non-Arrhenius behavior. Detailed examination of the SIA trajectories shows that SIA hops are correlated. At low temperature, the SIA has a higher probability of jumping back in the direction from whence it came, rather than forward along the same trajectory. At high temperatures, by contrast, this effect appears to be reversed. We quantified this observation by measuring a correlation factor for SIA diffusion, f , defined as

$$f = D/D_b, \quad (3)$$

where D_b is the "bare" diffusion constant given by $D_b = \bar{l}^2 n / 6$. Here, n is the average number of jumps per second and \bar{l} is the average jump length. For diffusion on a lattice, one can simply count the number of jumps per unit time and set \bar{l} equal to the nearest neighbor spacing $r_0 = \sqrt{3}/2a_0$. This procedure works well for single SIAs ($n = 1$) which are well localized on ideal lattice sites (see

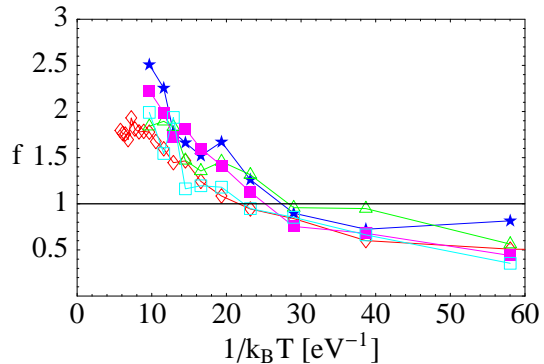


FIG. 8: Variation of the correlation factor f with $1/k_B T$ for single SIAs (\diamond) as well as clusters of size $n = 7$ (\star), $n = 19$ (\triangle), $n = 37$ (\blacksquare) and $n = 61$ (\square).

Fig. 3), but not for the continuous trajectories of the SIA clusters. In this case, one can still measure correlations on the scale of the nearest neighbor distance by dividing up the (continuous) trajectory into segments of equal length. In the present case, we determined n by counting the number of times the magnitude of the center of mass displacement exceeded $0.75r_0$. From this criterion, we measured \bar{l} by averaging over the actual displacements (in general $\bar{l} > 0.75r_0$ due to discrete recording of the trajectory). This procedure can be applied to both the single SIA trajectories as well as the clusters. We verified that for discrete trajectories of the single SIAs, it gives the same result as direct counting of the number of jumps.

Figure 8 shows the variation of the correlation factor, f , as computed by Eq. (3) for single SIAs and SIA clusters with $1/k_B T$. A value of $f = 1$ indicates an uncorrelated random walk. We observe that at low temperatures $T \leq 600$ K the migration is anticorrelated ($f < 1$), but rises quickly above one as T increases. This effect is most pronounced for single SIAs; for clusters, the values of f tend to be larger. The underlying physics leading to the T-dependent correlation factor is not obvious. One possibility is incomplete local relaxation leading to a memory effect. Once a SIA jumps to a neighboring site, the potential well to move back or move forward is not same if the atoms surrounding the SIA do not fully relax following SIA migration. In this case, the potential barrier for moving back to the original site is lower than barriers for other jumps. As the temperature increases, the thermal fluctuations will smear out this small difference between relaxed and unrelaxed environments, thereby erasing the memory effect. Once several SIAs come together to form a cluster, the trend towards anticorrelations seems to be weakened.

The impact of the correlations on the diffusivities can be isolated by plotting a "corrected" diffusivity, $\tilde{D} = D/f$ vs. $1/k_B T$ in Fig. 9. Now we see that for the single SIAs (\diamond), the low temperature data ($T \leq 500$ K) lie along a nearly straight line with slope $\Delta E_d = 0.018$ eV. The

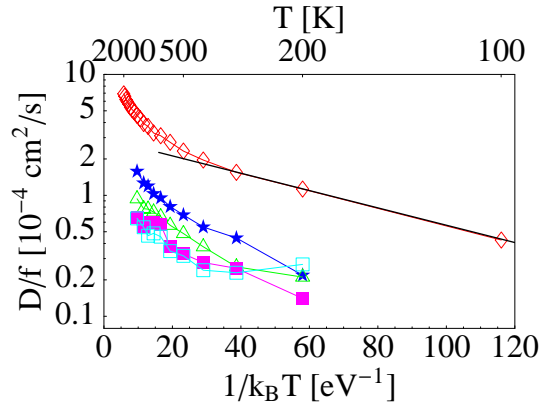


FIG. 9: Plot of the corrected diffusivities $\tilde{D} = D/f$ as a function of inverse temperature $1/k_B T$. The straight line is an Arrhenius fit to the lowest temperature data (see Fig. 8) and has slope $\Delta E_d = 0.018\text{eV}$.

temperature dependent correlation factor hence provides a partial explanation for the relatively weak deviations from Arrhenius behavior at low T . For the SIA cluster ($n > 1$), even the corrected diffusivities don't show a clear Arrhenius behavior at low T and no simple Arrhenius fit is possible. In all cases, significant non-Arrhenius behavior remains at higher T .

B. Diffusion over small barriers

As the temperature is increased beyond 300 K, the correlation factor rises quickly to a value greater than unity. These strong positive correlations signal that the SIAs hop easily over several barriers without completely thermalizing between hops. At the same time, we note that the energy barrier ΔE_d obtained in the low temperature regime (where an Arrhenius fit was possible) is smaller than the thermal energy for all but the two lowest temperatures studied here. This is likely the source of the multiple interstitial hops at high T . The small amplitude of the potential energy landscape does not localize the SIAs at the bottom of the potential well, but instead the atoms spend significant time in a wide range of positions in the landscape (i.e., the interstitial positions are delocalized). In conventional derivations of activated escape over barriers [44], however, one assumes that a well defined separation of time scales exists, in which the atoms spend most of their time near the energy minimum. The time required for crossing the barrier is assumed to be much smaller than the SIA residence time in individual minima. This scenario requires that $\Delta E_d \gg k_B T$, which is clearly not the case here.

It is therefore natural to expect a breakdown of the Arrhenius description in the present system. In the limit that the barrier height is completely negligible relative to the energy of the heat bath (the free particle limit),

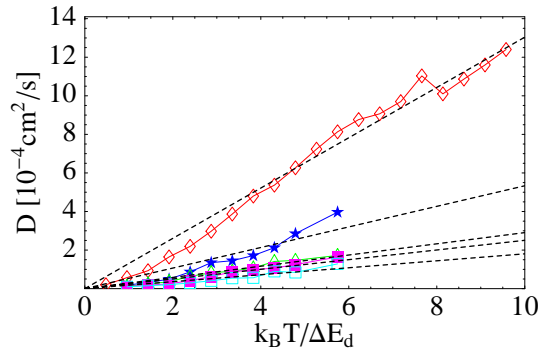


FIG. 10: Plot of the diffusivities as a function of temperature on a linear scale for single SIAs (\diamond) as well as clusters of size $n = 7$ (\star), $n = 19$ (\triangle), $n = 37$ (\blacksquare) and $n = 61$ (\square). The dashed lines indicate linear fits to the functional form $D = c_n T$.

simple arguments predict

$$D = k_B T / m \gamma, \quad (4)$$

where m is the mass of the particle and γ a relaxation time scale associated with a velocity-dependent friction force. This type of diffusion is typical for Brownian particles, e.g. colloids in solution, where the solvent provides a thermal bath. Since this free particle diffusion coefficient is expected to be a linear function of T , we replot the data from Fig. 7 on a linear temperature scale in Fig. 10. In this representation, the single SIA data is indeed nearly linear, albeit with weak curvature at low temperature. For the SIA cluster, it is not possible to fully explore the high T regime beyond 1200K, since the cluster become unstable, but the available data is also well-fit by a linear diffusivity-time relation. This suggests that SIA diffusion in V is free particle like at high temperature ($D \sim T$), but follows the normal Arrhenius, hopping dynamics at low T ($D \sim e^{-\Delta E_D / k_B T}$). The deviation from linearity at low temperature and the deviation from Arrhenius behavior at high temperature suggests that a cross-over occurs between the free ($k_B T \gg \Delta E_D$) and hopping particle ($k_B T \ll \Delta E_D$) limits.

No simple analytic theory exists that addresses the behavior in the transition regime. We therefore proceed by considering a simplified one-dimensional model with a particle of mass m that diffuses in a sinusoidal potential. The dynamics of this particle is described by the Langevin equation

$$m\ddot{x} - \gamma\dot{x} = \epsilon/2 \cos[x/\sigma] + \eta, \quad (5)$$

where η is a white noise term that is proportional to temperature (the prefactor is easily determined from the fluctuation-dissipation theorem). By solving this equation numerically for different potential amplitudes ϵ , we can continuously move between the two limiting cases of strong and weak barriers. Figure 11(a) shows the result of the numerical solution to this model in an Arrhenius plot, where it yields a straight line when T is much

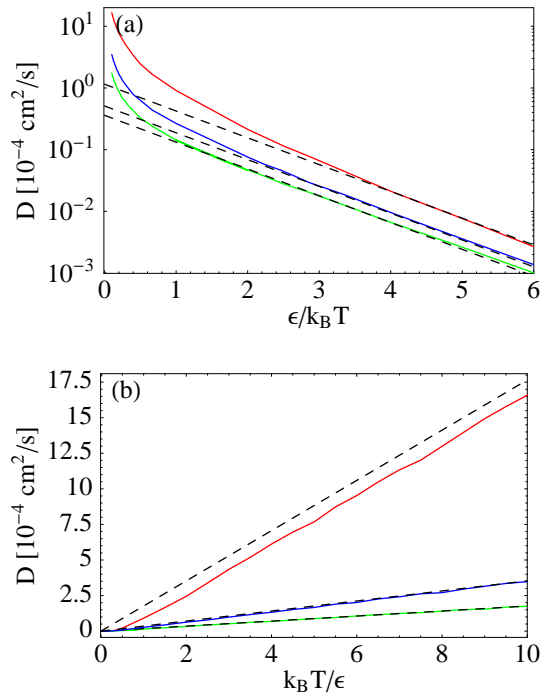


FIG. 11: Diffusivity of a one-dimensional Brownian particle in a sinusoidal potential of amplitude ϵ for three values of the damping parameter $\gamma = 1\tau^{-1}, 0.2\tau^{-1}$ and $0.1\tau^{-1}$. $\tau = \sqrt{m\sigma^2/\epsilon}$ is the intrinsic timescale of the model. The diffusivity decreases with increasing γ . The Arrhenius representation ($1/T$) (a) yields a straight line at large values of $(\epsilon/k_B T)$, while the linear temperature plot (b) exhibits a straight line in the opposite limit. Solid lines numerical solution of Eq. (5), dashed lines Arrhenius and free particle limits, respectively. The model maps onto realistic length and time scales for V after insertion of values for m and σ .

smaller than ϵ , followed by strong deviations from this line at higher T , as observed in the MD simulations. In Fig. 11(b) we plot the same data as a linear function of T and obtain a straight line as soon as the thermal energy is larger than the barrier height. This simple model successfully captures both limiting cases. The crossover temperature from the particle hopping to free particle behavior depends on the precise value of the damping parameter γ . The model can be mapped onto the full MD results after inserting values of m and σ for V and setting $\epsilon = \Delta E_d$. This excellent agreement between the MD results and model predictions demonstrates that the observed strongly non-Arrhenius interstitial diffusion in V is a direct consequence of the relative magnitudes of the activation energy and the thermal energy.

C. Scaling of the prefactor

According to Fig. 10, the diffusivities for all cluster sizes n can be described as a linear function of temperature, i. e., $D = c_n T$. The dependence of the diffusivity on

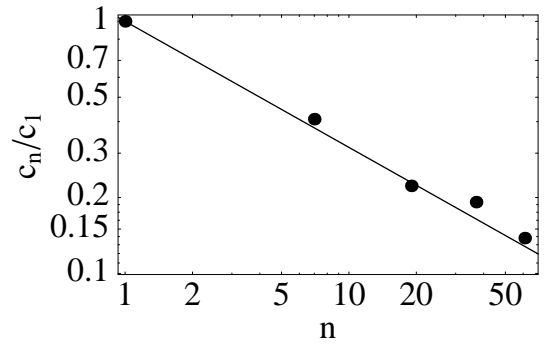


FIG. 12: Scaling of the prefactor c_n with cluster size n , normalized by the prefactor for $n = 1$. The straight line shows a power law function n^α , with an exponent $\alpha = -0.5$.

cluster size is now captured by the size-dependent prefactor c_n . This prefactor exhibits an interesting scaling with n . Fig. 12 plots c_n as a function of n in a double-logarithmic plot. The data fall along a straight line that is consistent with a simple power law $c_n/c_1 = n^\alpha$, where $\alpha = -0.5$. The same factors c_n/c_1 could also be used to collapse the Arrhenius plots of Fig. 7 onto a single curve. As discussed below, such a power law scaling of prefactors with cluster size has been previously observed in simulations of other systems [43]. At present, no satisfying explanation for this intriguing observation is available.

VI. DISCUSSION AND CONCLUSIONS

This paper presents the results of a series of molecular dynamics simulations of diffusion of self-interstitial atoms and self-interstitial clusters in vanadium. The computations used an improved FS-type interatomic potential that correctly reproduces the $\langle 111 \rangle$ self-interstitial as the lowest energy interstitial configuration. Single self-interstitials migrate easily along $\langle 111 \rangle$ -directions via a crowdion mechanism, and can also rotate into other $\langle 111 \rangle$ -directions with a much lower frequency. The rotations follow simple Arrhenius behavior and the rotation barrier is $\Delta E_r = 0.44\text{eV}$. SIA cluster do not rotate on the time scale of the present simulations, but rather move along a one-dimensional path.

Diffusivities were determined over a wide temperature range (100K-2000K for single SIAs, 200K-1200K for SIA cluster) for several SIA cluster sizes $n = 1, 7, 19, 37, 61$. For all cluster sizes, the diffusivities exhibit strongly non-Arrhenius behavior. A correlation analysis revealed that the motion of the SIAs is anticorrelated at the lowest temperatures, but develop very strong positive correlations at higher T . An estimate of the activation barrier at low T yielded the very low value of $\Delta E_d = 0.018\text{eV}$, a value smaller than most thermal energies employed in this study. The role of the energy barrier is therefore small compared to the thermal energy above room temperature, and the non-Arrhenius behavior arises from a

crossover to nearly free particle diffusion, where the diffusivity varies linearly with T . It is imperative to examine a sufficiently wide temperature range to properly identify this transition.

The present results indicate that the energy barrier for SIA motion is very small and is only weakly dependent on cluster size n . This follows from the fact that diffusivities versus temperature curves can be superposed by a linear shift in an Arrhenius plot, or alternatively, that the diffusivities of the clusters are all linear functions of temperature, albeit with size-dependent slopes. In V, SIA diffusivities are therefore better described in a nearly free particle picture, in which the functional form obeys the relation $D = c_n T$. The prefactors c_n obey a simple power law scaling with system size.

Interesting parallels can be drawn between our study on vanadium and results for iron. Osetsky *et al.* [43] studied the diffusive motion of SIA clusters in Fe for sizes between $n = 1$ and $n = 91$ and also found that the ac-

tivation energy varies weakly with temperature. In their study, the diffusivities are fit to Arrhenius expressions, but the temperature range is much smaller than here. As in V, the size dependence of the diffusivities could be absorbed in a prefactor which also exhibits power law scaling, but with a different exponent $\alpha = -0.64$. The power law scaling seems to be generic to the motion of dislocation loops and calls for further studies.

VII. ACKNOWLEDGEMENTS

We thank G. H. Gilmer, and J. A. Caro for useful discussions. This work was performed under the auspices of the U.S. Department of Energy, Office of Energy Sciences (DE-FG02-01ER54628) and Lawrence Livermore National Laboratory under Contract No. W-7405-Eng-48.

-
- [1] Young FW. J. Nucl. Mater. 1978;69:310.
 - [2] Young FW, Cost JR, Nowick AS, Stiegler JO. Mater. Sci. Eng. 1978;35:91
 - [3] Nordlund K, Keinonen J, Ghaly M, Averback RS. Nature 1999;398:49.
 - [4] Chung HM, Loomis BA, Smith DL. J. Nucl. Mat. 1996;239:139.
 - [5] Chung HM, Loomis BA, Smith DL. Fusion Eng. Des. 1995;29:455.
 - [6] Smith DL, Chung HM, Loomis BA, Matsui H, Votinov S, Vanwittenburg W. Fusion Eng. Des. 1995;29:399.
 - [7] Zinkle SJ, Matusi H, Smith DL, Rowcliffe AF, van Osch E, Abe K, Kazakov VA. J. Nucl. Mat. 1998;263:205.
 - [8] Osetsky YN, Victoria M, Serra A, Golubov SI, Priego V. J. Nucl. Mat. 1997;251:34.
 - [9] Osetsky YN, Serra A, Singh BN, Golubov SI. Phil. Mag. A 2000;80:2131.
 - [10] Díaz de la Rubia T, Guinan MW. Phys. Rev. Lett. 1991;66:2766.
 - [11] Foreman AJE, English CA, Pythian WJ. Phil. Mag. A 1992;66:655.
 - [12] Bacon DJ and Díaz de la Rubia T. J. Nucl. Mat. 1994;216:275.
 - [13] Minashin AM, Ryabov VA. J. Nucl. Mat. 1996;233:996.
 - [14] Morishita K, Sekimura N, Díaz de la Rubia T. J. Nucl. Mat. 1997;248:400.
 - [15] Morishita K and Díaz de la Rubia T. J. Nucl. Mat. 1999;272:35.
 - [16] Morishita K, Díaz de la Rubia T, Alonso E, Sekimura N, Yoshida N. J. Nucl. Mat. 2000;283:753.
 - [17] Morishita K, Díaz de la Rubia T, Kimura A. Nucl. Instr. Meth. Phys. Res. B 2001;180:66.
 - [18] Han S, Zepeda-Ruiz LA, Ackland GJ, Car R, Srolovitz DJ. Phys. Rev. B 2002;66:220101.
 - [19] Han S, Zepeda-Ruiz LA, Ackland GJ, Car R, Srolovitz DJ. J. Appl. Phys. 2003;93:3328.
 - [20] Zepeda-Ruiz LA, Rottler J, Han S, Ackland GJ, Car R, Srolovitz DJ, Phys. Rev. B 2004;70:060102(R).
 - [21] Car R, Parrinello M. Phys. Rev. Lett. 1985;55:2471.
 - [22] Finnis MW and Sinclair JE. Phil. Mag. A 1984;50:45.
 - [23] Daw M and Baskes MI. Phys. Rev. B 1984;29:6443.
 - [24] Johnson RA and Oh DJ. J. Mater. Res. 1989;4:1195.
 - [25] Foiles SM and Daw M. Phys. Rev. B 1988;38:12643.
 - [26] Adams JB, Foiles SM. Phys. Rev. B 1990;41:3316.
 - [27] Wirth BD, Odette GR, Maroudas D, Lucas GE. J. Nucl. Mat. 1997;244:185.
 - [28] Wirth BD, Odette GR, Maroudas D, Lucas GE. J. Nucl. Mat. 2000;276:33.
 - [29] Carlberg MH, Münger EP, Hultman L. J. Phys-Condens Matt 2000;276:33.
 - [30] Díaz de la Rubia T, Guinan MW. J. Nucl. Mat. 1990;174:151.
 - [31] Guinan MW, Stuart RN, Borg RJ. Phys. Rev. B 1977;15:699.
 - [32] Klabunde CE, Redman JK, Southern AL, Coltman Jr. RR. Phys. Stat. Sol. A 1974;21:303.
 - [33] Coltman Jr. RR, Klabunde CE, Redman JK, Williams JM. Rad. Eff. 1975;24:69.
 - [34] Segel V, Pelleg J. Phil. Mag. A 1997;76:1203.
 - [35] Ullmaier H, ed. *Atomic Defects in Metals*, Landolt-Börnstein series, vol. III/25. Berlin: Springer, 1991.
 - [36] Soneda N and Díaz de la Rubia T. Phil. Mag. A 1998;78:995.
 - [37] Gao G, Bacon DJ, Osetzky YN. J. Nucl. Mat. 2000;276:213.
 - [38] Osetsky YN, Priego V, Serra A. J. Nucl. Mat. 2000;276:202.
 - [39] Pasianot RC, Monti AM, Simonelli G, Savino EJ. J. Nucl. Mat. 2000;276:230.
 - [40] Marian J, Wirth BD, Perlado JM, Odette GR, Díaz de la Rubia T. Phys. Rev. B 2001;64:094303.
 - [41] Tully JC, Gilmer GH, Shugard M. J. Chem. Phys. 1979;71:1630.
 - [42] Zepeda-Ruiz LA, Marian J, Wirth BD. Phil. Mag., in press.
 - [43] Osetsky YN, Bacon DJ, Serra A, Singh BN, Golubov SI, Phil. Mag. 83, 61 (2003)
 - [44] Haenggi P, Talkner P and Borkovec M, Rev. Mod. Phys.

